Enhanced Compaction of Porous Sandstone Deformed Under High Confining and Pore Fluid Pressures

Olayinka Koso-Thomas

GEOL394

Advisors:

Dr. Wenlu Zhu
Zachary Zega

April 25th, 2023

Table of Contents

Abstract

Brittle deformation at varying differential pressures for porous rocks has been an object of study in rock deformation for years but continues to have areas of research that are under-investigated. This paper explores whether varying the pore fluid pressure at a constant differential pressure during deformation systematically affects the degree of compaction and inelastic behavior of the sample, resulting in behavior supported or divergent to the effective stress law. Axial deformation experiments were performed on porous Adamswiller sandstone (~23-25% initial porosity) under various confining and pore fluid pressures. The degree of compaction and dilatancy in Adamswiller samples deformed under a differential pressure of 10 MPa did not systematically vary as a function of the pore fluid pressure, which is in accordance with the effective stress law. However, Adamswiller sandstone deformed at a differential pressure of 20 MPa showed enhanced compaction under conditions of high pore fluid pressure relative to those samples deformed at lower values of pore fluid pressure, which is in apparent contradiction to the effective stress law.

Initial qualitative microstructural analysis of an enhanced compactant sample at high pore fluid pressure showed less damage in comparison to a dilatant sample at low pore fluid pressure. Higher normal stress within grains at higher confining and pore fluid pressures could be a possible reason for the difference in damage seen in the enhanced compaction sample, but more quantitative analysis could elucidate other conclusions from the microstructures.

This paper documents that conditions of high confining and pore fluid pressures can systematically result in enhanced compaction relative to samples deformed at lower values of confining and pore fluid pressures. These results have critical implications for those who wish to exploit sandstone reservoirs more effectively for economic activities such as carbon sequestration, wastewater disposal, and hydraulic fracturing.

Plain language abstract

Understanding the deformation of porous rocks under upper-crustal conditions is critical for economic activities like oil and gas extraction. Rock deformation experiments are performed to create analog situations that can be applied to natural conditions. During these experiments, porous rocks are subjected to realistic pressure conditions by applying confining pressure, and pore fluid pressure, which is applied to the sample because natural rocks are often fluid-saturated. Porous rocks such as sandstones may experience varying degrees of compaction (volume decrease) or dilatancy (volume increase) while deforming. The relative amount of dilatancy and compaction of inelastically deforming rock is thought to be controlled by the effective stress, which is the difference between the normal stress and the pore fluid pressure. Experimentally, the effective stress depends on the applied differential pressure, or the difference between the confining and pore fluid pressures.

Prior experimental work demonstrates that porous sandstones deformed at higher differential pressures generally experience more overall compaction due to pore collapse and grain crushing, whereas sandstones deformed at lower differential pressures experience more overall dilatancy in the absence of processes leading to compaction. Because the deformation of porous rocks is assumed to obey the effective stress law, prior experimental work does not constrain the effect of pore fluid pressure on the inelastic behavior of porous sandstones. For instance, it is currently unclear whether varying pore fluid pressure while maintaining constant differential

pressure affects the degree of compaction in fluid-saturated rock. This paper demonstrates the inelastic behavior of porous Adamswiller sandstone at constant differential pressures and varying pore fluid pressures.

1. Introduction and Background

1.1. Sandstone reservoirs and laboratory experiments

Sandstones are important reservoirs in Earth's upper crust, allowing for storage of economically vital material, such as oil and gas. Natural conditions at depth supply pressure and stresses from overlying rock, or overburden pressure, causing a decrease in available pore space within the reservoir, altering the physical properties of the rock. To understand deformation of sandstones in a natural setting, laboratory experiments apply realistic pressure conditions via a deformation apparatus to sandstone samples while collecting mechanical data on the deforming rock.

Upper-crustal rocks are in the brittle regime, so processes that affect rock deformation are also considered brittle deformation. These rocks can experience deformation via microcracking, grain crushing, and pore collapse, all in the brittle regime. Dilation, or dilatancy, is the increase of space within a grain or crystalline rock by way of cracking, such as microcracks and microfractures (Brace, 1978). Compaction is the decrease of pore space and volume in the sample through processes like grain crushing or pore collapse (Brace, 1978).

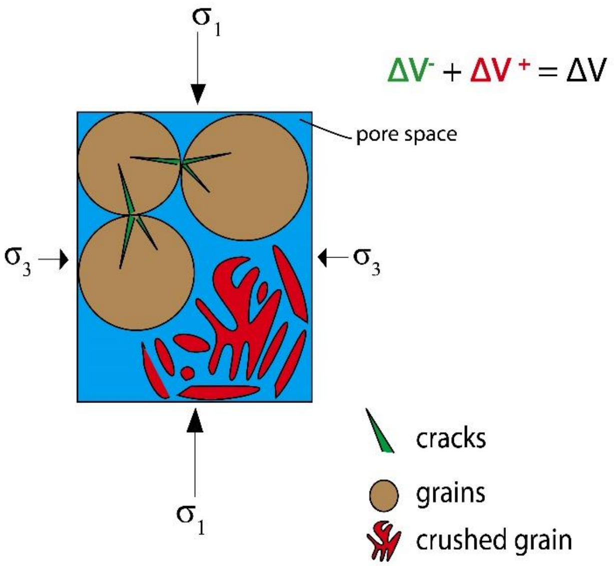

Fig. 1 Graphic of micromechanisms during compaction of a sandstone with principal stresses σ_1 (vertical) and σ_3. Grain contacts would nucleate microcracks (green). Crushed grains (red) would result from numerous micro-cracks in a grain. Microcracks would decrease the bulk change in volume (ΔV^-). Crushed grains would increase the bulk change in volume (ΔV^+).

Volume change during deformation of sandstone samples can either be negative or positive (**Fig. 1**). A negative volume change indicates the sample's dilatant processes dwarfed the compactant processes during the deformation experiment, where dilatancy is a volume increase resulting in a lower volume change from the initial volume; a positive volume change indicates compaction, where compactant processes, such as pore collapse and grain crushing dwarfed the dilatant processes throughout the deformation experiment, resulting in a higher volume change from the initial volume. (Brace 1978).

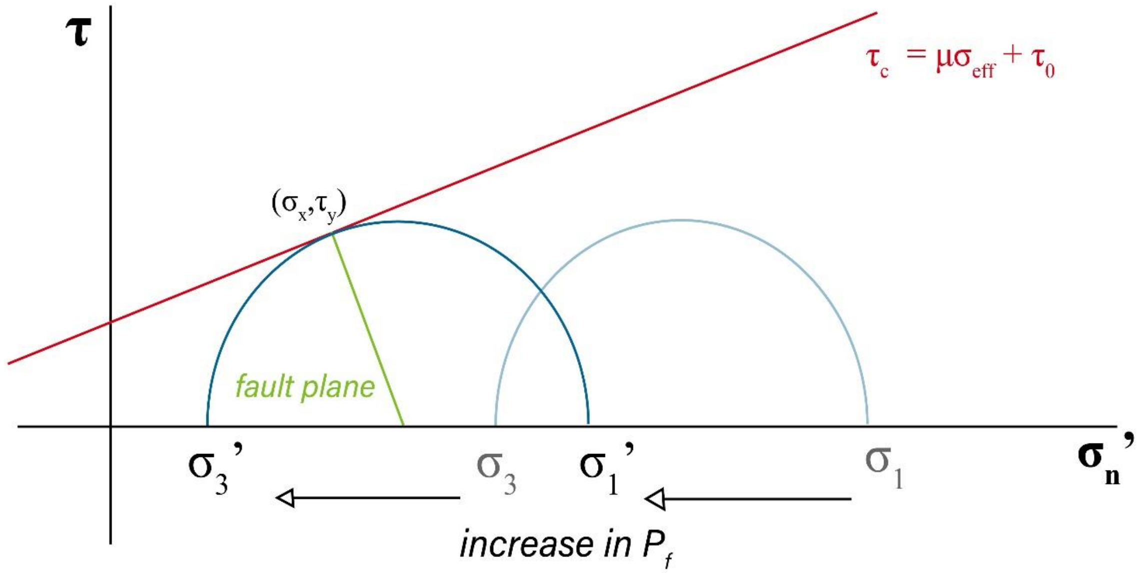

Fig. 2 A Mohr's circle for an arbitrary fault plane after an increase in the pore fluid pressure. (σ_x,τ_y) is the intersection between the Coulomb failure criterion and the Mohr's circle where the rock will fail. σ_1 and σ_3 are shifted towards the failure criterion line as pore fluid increases

1.2. Importance of the effective stress law

As the dilatancy and compaction affect the volume change during deformation, other factors, such as fluid pressure, can affect the sample's strength. In the case of fluid-saturated rock, the strength of the rock is determined by the effective normal stress σ_{eff}, not the total normal stress σ_n. During deformation, the stress on any plane in the sample can be defined by the effective stress law, where σ_n is the normal stress, P_f is the pore fluid pressure and σ_{eff} is the effective stress:

$$\sigma_{eff} = \sigma_n - P_f \qquad (1)$$

The effective stress law describes the total stress on a plane as the total normal stress acts perpendicular to the plane and the pore fluid pressure acts isotopically, counteracting the applied normal stress (Nur and Byerlee, 1971). If the effective stress remains constant, inelastic behavior of the sample during deformation should be the same regardless of high or low values of pore fluid pressure and normal stress.

When increasing pore fluid pressure under a constant total normal stress σ_n, the sample weakens due to the counteracting pore fluid pressure, causing faults and sample failure. The sample failure is controlled by the failure criterion τ_c of the rock as well as the effective stress, failure coefficient μ, and the initial rock strength τ_0 through the failure criterion equation:

$$\tau_c = \mu\sigma_{eff} + \tau_0 \qquad (2)$$

The sample will fault at a lower effective stress due to a lower failure criterion when there is increased pore fluid pressure, resulting in a weaker rock sample overall (**Fig. 2**).

In addition to the effective stress law, samples will undergo changes in differential pressure P_{dif}, defined as the difference between the confining pressure P_c and the pore fluid pressure:

$$P_{dif} = P_c - P_f \qquad (3)$$

The differential pressure directly controls the effective stress state in the rock, where the confining pressure works as the normal stress on a grain and the pore fluid pressure acts isotopically. By adjusting the differential pressure, certain rock deformation experiments can test the effective stress law on sandstones and draw conclusions about inelastic behavior of porous rocks during deformation.

1.3. Past work involving sandstones and the effective stress law

Past experiments by Wong et al. (1997) investigated the transition between brittle faulting and cataclastic flow in sandstones, where they analyzed and performed axial deformation experiments on Adamswiller sandstone. Wong et al. (1997) constructed a plot of porosity change, an equivalent to volumetric strain, throughout the samples as differential pressure was increased and showed that samples at lower differential pressures experienced more dilatancy and the samples at higher differential pressures compacted throughout the entire experiment. Wong et al. (1997) used various sandstones, including Adamswiller sandstone, but kept their pore fluid pressure value the same at 10 MPa as the confining pressure was increased.

Within the large quantity of experimental work on porous rock deformation (Dropek et al. 1978; Menendez et al. 1996; Wong et al. 1997), it is a general consensus that porous rocks have more dilatant behavior below differential pressures of 30 MPa and more compactant behavior above 100 MPa (Wong and Baud, 2012). As mentioned previously with Wong et al. (1997), the pore fluid pressure was held constant at 10 MPa as the confining pressure was increased. This approach fails to acknowledge that the pore fluid pressure can be varied. A different application of equation (3) would entail varying the pore fluid pressure as the differential pressure remains the same.

1.4. Hypothesis

Using Adamswiller sandstone, the effective stress law can be tested with varying pore fluid pressures that can support either the null or the alternative hypothesis, respectively:

(1) If the pore fluid pressure is varied at a constant differential pressure and follows the behavior described by the effective stress law, then the deformation and degree of compaction for Adamswiller sandstone should be similar at both high and low confining and pore fluid pressures.

(2) If the pore fluid pressure is varied at a constant differential pressure and does not follow the behavior described by the effective stress law, then the inelastic behavior of the sample will vary as the confining and pore fluid pressures are varied. In this situation, differences in micromechanisms, such as grain crushing, pore collapse, and microcracking, could be the reason for the change in deformation behavior.

2. Methods and Materials

2.1. Adamswiller sandstone

Experiment #	Pc (MPa)	Pf (MPa)	Differential Pressure (MPa)	Initial porosity (%)	Notes
H167-A7b	130	120	10	--	
H168-A8b	12	2	10	25	
H169-A2a	190	180	10	25	
H171-A3a	190	180	10	26	Closed valve during experiment
H172-A4a	190	180	10	24	
H173-A5a	12	2	10	24	
H174-A6a	160	150	10	24	
H175-A7a	70	60	10	24	
H177-A9a	130	120	10	24	
H179-A11a	40	10	30	24	
H180-A12a	30	10	20	24	
H181-A14a	190	170	20	25	Thin section sample
H182-A15a	130	110	20	24	
H183-A16a	130	110	20	25	
H184-A17a	170	150	20	24	Initially 190/170, electrical issue
H185-A18a	30	10	20	23	
H186-A19a	30	10	20	23	Thin section sample

Table 1. Adamswiller sandstone experiments at differential pressures of 10 MPa, 20 MPa, and 30 MPa with porosity values for this paper. All experiments in this table were performed under conditions for testing the previously mentioned hypothesis. Thin section samples chosen are noted.

Cylindrical samples from the Adamswiller sandstone formation are cut at ~18 mm in diameter and ~38 mm in length. The initial porosity is calculated after the sample is dried under vacuum at 30 °C for >12 hours, before being submerged in water under vacuum for >12 hours, with weight measurements noted after drying and wetting the sample. The initial porosity ranges between ~23-26% (**Table 1**).

2.2. Deformation experiments

Laboratory experiments can recreate subsurface conditions for sandstone reservoirs, with added principal stresses – σ_1 and σ_3, where $\sigma_1 > \sigma_3$ – and pressures resembling natural conditions. Axial deformation experiments place the sample under the natural pressure conditions in question before increasing the σ_1 stress for deformation of the rock via an axial load (**Fig. 3a**). σ_3 is kept constant throughout the experiment and σ_2 is equated to σ_3. The differential stress σ_1 on the sample is defined as:

$$\Delta\sigma = \sigma_1 - \sigma_3 \qquad (4)$$

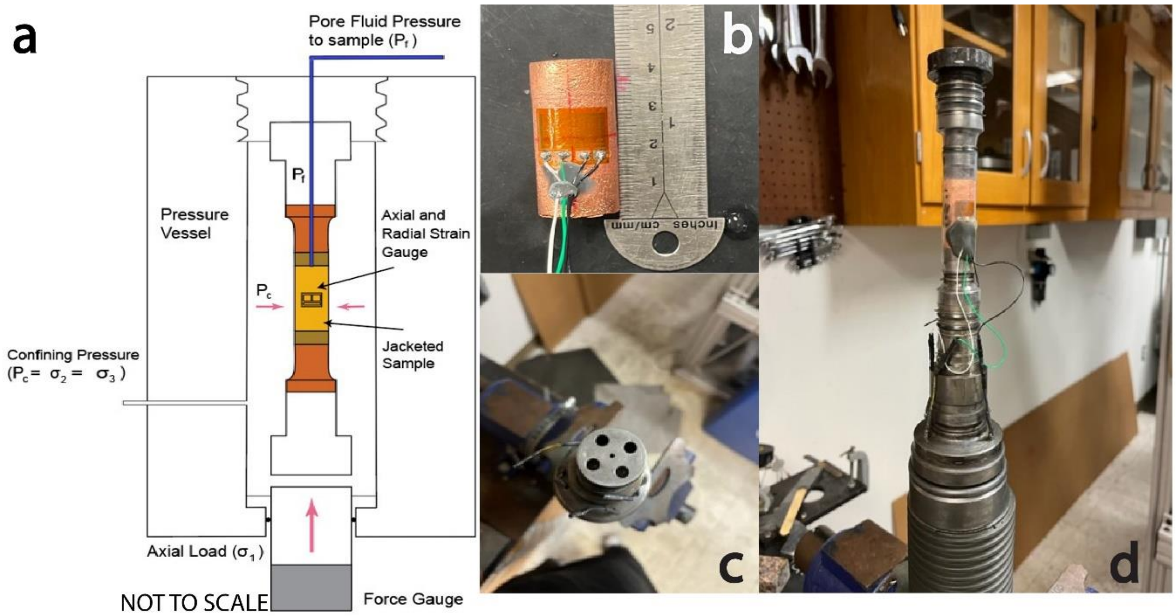

Fig. 3 (a) Cross-section of hot press, (b) Adamswiller sandstone covered with copper jacket and strain gauge with wires, (c) pore fluid tube on base plug, and (d) full sample attached to base plug

Because the differential pressure on a rock is directly related to the effective stress, these rock deformation experiments keep the differential pressure constant to analyze how the effective stress law applies to rocks. Axial deformation applies pressures directly related to differential pressure and subsequently, the effective stress law (Zhang et al. 1990).

To conduct the experiments, Adamswiller sandstone samples were axially deformed by the hot press apparatus (**Fig. 3a**). Before running the experiment, the sample was sealed inside a vacuum at ~30 °C for >12 hours to dry. The sample was weighed three times before being put under vacuum again and submerged into distilled water simultaneously. To allow for complete saturation of the sample, it was left for >12 hours in the water and weighed three times before sample assembly. A copper jacket was compacted onto the sample where a strain gauge was attached to measure bulk sample deformation during the experiment (**Fig. 3b**). A polyolefin jacket was heat-shrunk onto the sample with the strain gauge before being loaded into the hot press (**Fig. 3d**). The samples were pressurized within a confining medium of kerosene and pore fluid was added via a pore tube through the top of the hot press (**Fig. 3c**).

The sample was pre-compacted for a minimum of 1 hour to equilibrate the fluid before increasing the confining and pore fluid pressure in a stepwise manner to the experimental conditions, keeping a constant differential pressure throughout. Once experimental conditions are reached, the axial load is raised and deforms the sample at a strain rate of 10^{-6} s^{-1} until the sample reaches peak stress, a stress drop, and subsequent frictional sliding. Samples are unloaded before the frictional sliding breaks through the polyolefin jacket and before excessive damage to the microstructure occurs.

Axial strain is calculated from the axial displacement monitored by a linear variable differential transformer (LVDT), similar to other methods for axial deformation experiments on porous sandstone (Menendez et al. 1996; Wong et al. 1997). The strain gauge takes measurements in the horizontal and vertical direction at 2 Hz, with a measurement in the horizontal and vertical direction twice every second. Volumetric strain was calculated using axial strain and radial strain was measured from the strain gauge on the copper jacket.

2.3. Thin sections for microstructures

Thin sections were made for samples H181-A14a and H186-A19a from the suite of experiments performed at a differential pressure of 20 MPa (**Table 1**). The samples were chosen based on visible fractures after removing the copper jacket as well as experimental results (experiments with electrical issues and skewed data or jacket leaks were not chosen). The samples were placed under vacuum before being submerged in epoxy so the pore space could be filled, and any microstructures preserved. The samples were then pre-cut with a rock saw along planes of interest that might show internal faults and damage. The samples were then sent to a manufacturer for 30 µm thick thin sections to be made.

3. Results

3.1. Axial deformation analysis

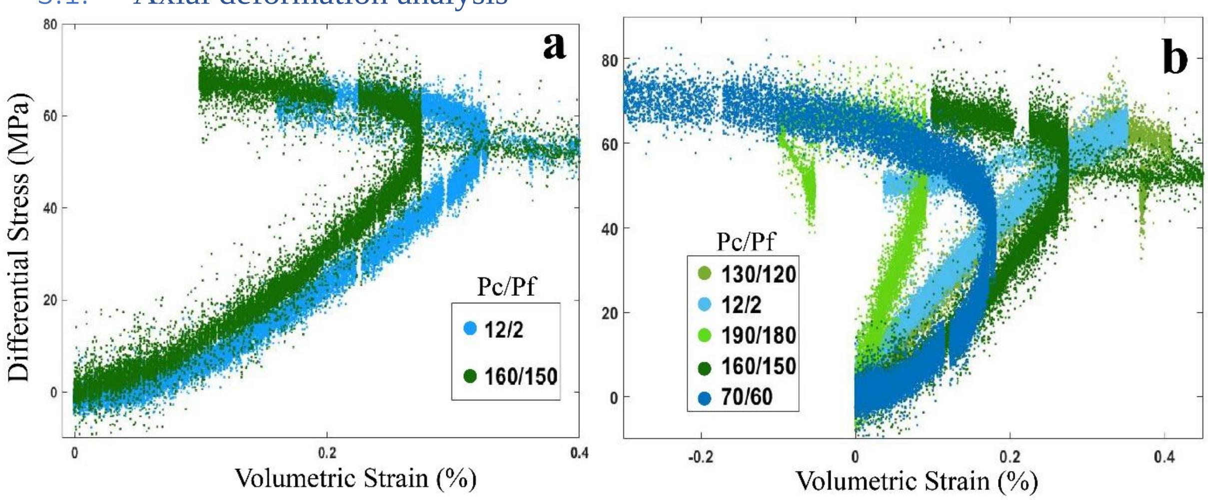

Fig. 4 Adamswiller sandstone deformed at a differential pressure of 10 MPa. (a) Volumetric strain plotted against differential stress of 160/150 (green) and 12/2 (blue). (b) Volumetric strain plotted against differential stress for a range of pore fluid pressures from low pore fluid pressure (blue) to high pore fluid pressures (green).

When analyzing volumetric strain curves (**Fig. 4**; **Fig. 5**), there is an initial crack closure, followed by quasi-elastic compaction where the curve is linear. Once the stress-strain curve becomes nonlinear, we can observe either shear-induced dilatancy with a negative volumetric strain, or shear-enhanced compaction with continued positive linear trend of volumetric strain. The rock will then fail and undergo a stress drop.

From the suite of experiments performed at a differential pressure of 10 MPa, the degree of compaction was similar for experiments performed at a low pore fluid pressure of 2 MPa and a higher pore fluid pressure of 150 MPa (**Fig. 4a**). The volumetric strain data from a range of pore fluid pressure from 2 MPa to 180 MPa showed no enhanced compaction when separated into experiments with higher and lower pore fluid pressures, and overall had no systematic degree of compaction or dilation in response to varying pore fluid pressures (**Fig. 4b**).

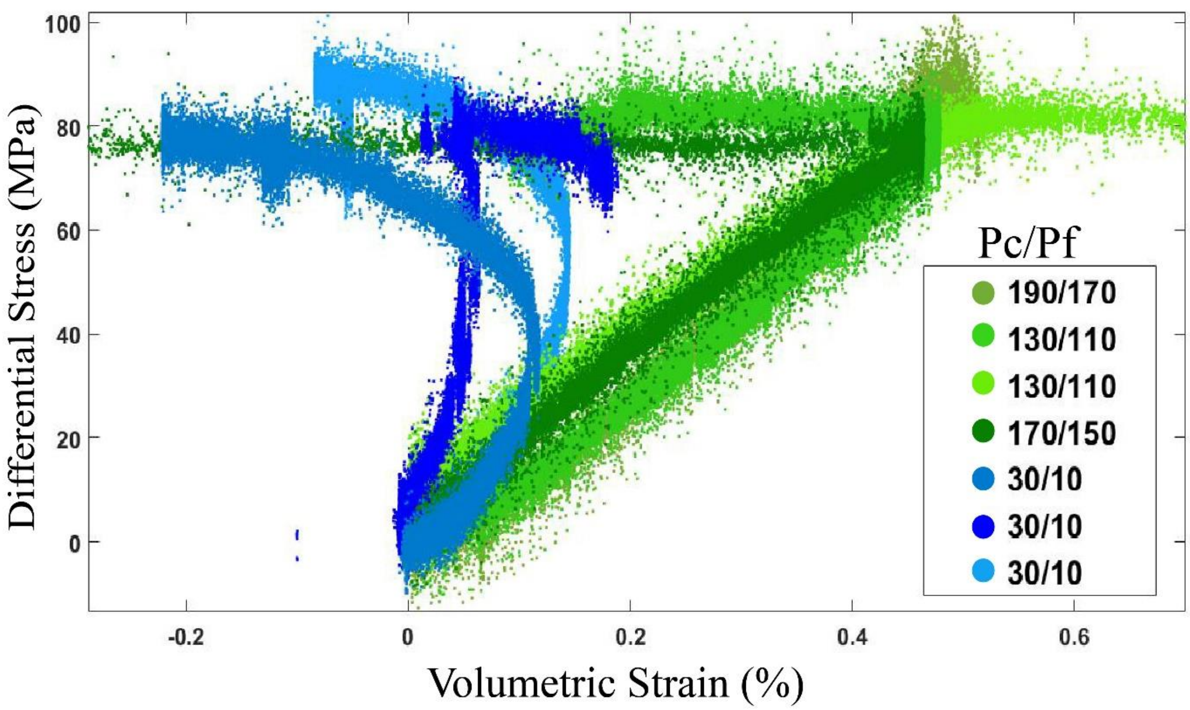

Fig. 5 Adamswiller sandstone deformed at a differential pressure of 20 MPa. Volumetric strain plotted against differential stress with high pore fluid pressures in green and low pore fluid pressures in blue.

From the suite of experiments performed at a differential pressure of 20 MPa, the degree of compaction was enhanced for the higher pore fluid pressure experiments and the dilatancy, although consistent with lower pore fluid pressure experiments, had sample variations (**Fig. 5**). Unlike the experiments done at a differential pressure of 10 MPa, the degree of compaction becomes consistent as higher pore fluid pressures are achieved. Experiments were reproduced and the enhanced compaction persisted.

3.2. Microstructural analysis

Precursory analysis of the thin sections chosen – high pore fluid pressure sample H181-A14a and low pore fluid pressure sample H186-A19a – showed more damage in the sample deformed at a low pore fluid pressure (**Fig. 6**). Qualitative differences between the samples show a more distinct and larger fault zone in the low pore fluid pressure sample (**Fig. 6a**) and less distinct and smaller fault zone in the higher pore fluid pressure experiment (**Fig. 6b**). Quantitative analysis involving grain damage counting is a possible avenue for further analysis of these thin sections.

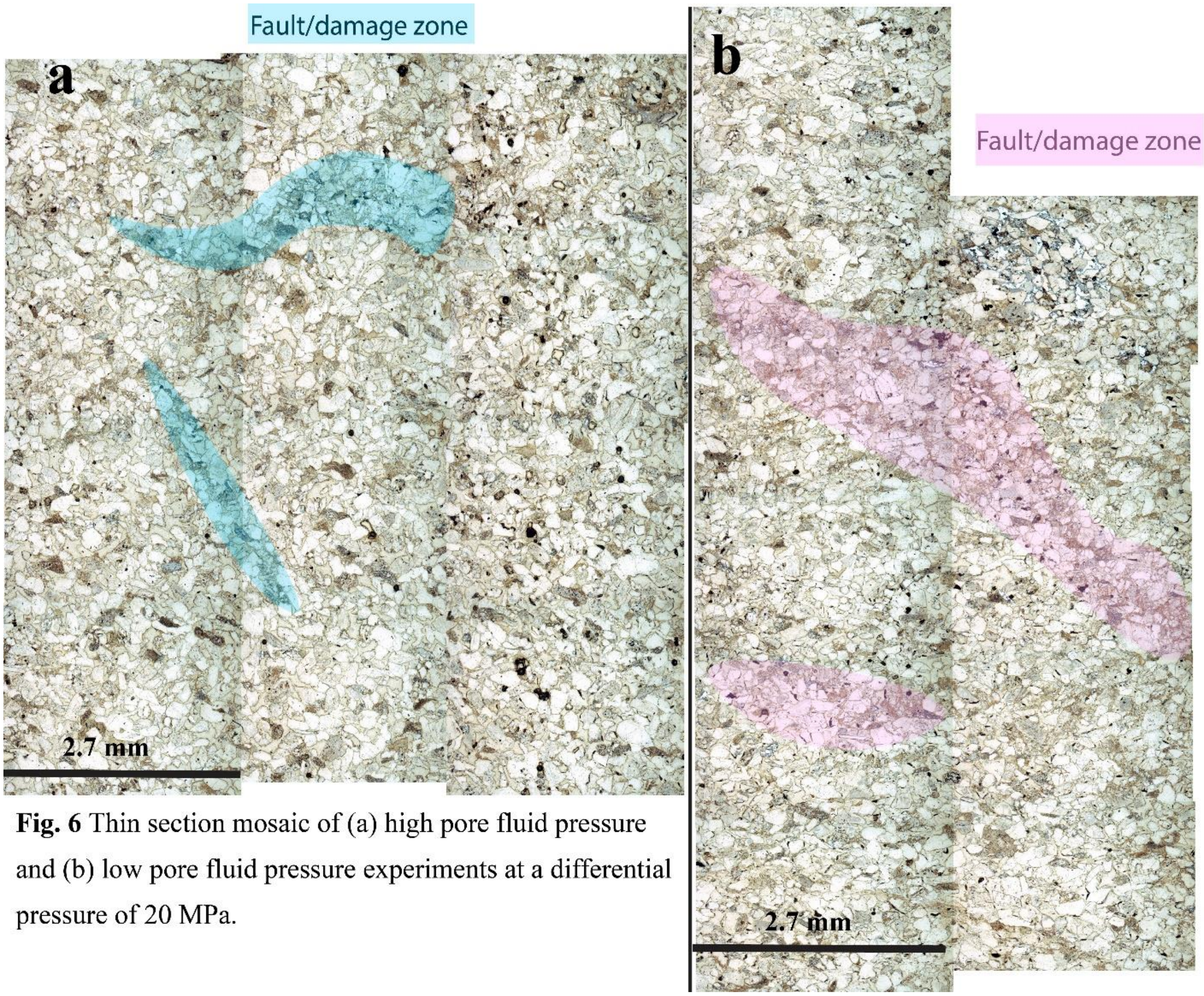

Fig. 6 Thin section mosaic of (a) high pore fluid pressure and (b) low pore fluid pressure experiments at a differential pressure of 20 MPa.

4. Discussion

4.1. High effective stress within grains

The enhanced compaction for the experiments seen at a differential pressure of 20 MPa (**Fig. 5**) cannot be explained by the effective stress law alone and bears no resemblance to the sample variations seen at a differential pressure of 10 MPa (**Fig. 4b**). The enhanced compaction could be a result of microcracks generated at grain contacts, but the thin section from an experiment with enhanced compaction shows less damage and faulting (**Fig. 6a**).

Grain compaction can occur as the pressure surrounding the grain increases, decreasing the size of the grain. The decreased grain size can allow for movement of the grain throughout the pore space but can also change the stress within the grain. Grain size reduction can result in a higher normal stress within the grain, and from equations (1) and (2), a higher normal stress means a higher strength grain (**Fig. 7**). The higher normal stress within the grain could cause less microcrack nucleation, causing less damage, and ultimately resulting in less faults. Previous experiments on other rock types have also found that higher confining pressures resulted in less observed microcracks nucleating at grain boundaries (Kranz, 1983).

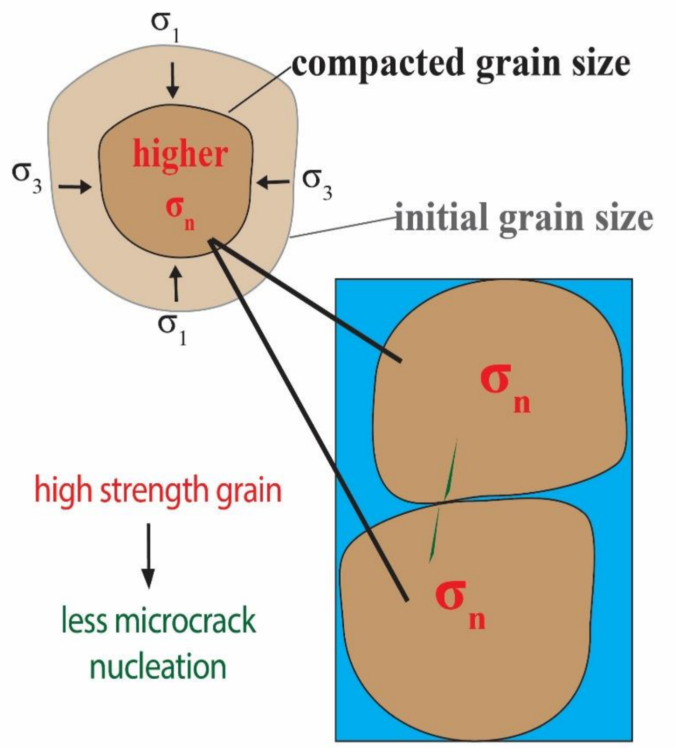

Fig. 7 Cartoon of possible increased normal stress within the grain, decreasing the microcrack nucleation.

The high pore fluid pressure experiments would experience this increased normal stress within the grain, but the low pore fluid pressure experiments would not have the strengthened grains and would experience more faulting.

4.2. Implications

Sandstones are important reservoirs for a number of resources, like oil and gas, and understanding their compactive behavior is crucial. Laboratory experiments for rock deformation, especially porous rocks, are vital in applications to these reservoirs, as the experimental conditions can be analogous to natural conditions. The loss of porosity in sandstone reservoirs due to compaction and grain realignment is an outcome that can affect the quality of the reservoir and whether it can be of use (Worden et al. 2018). Understanding the response of sandstone to environmental conditions like increased stress and pore fluid pressure can help with anthropogenic uses of sandstone reservoirs.

5. Conclusions

5.1. Summary

Previous work on the deformation of porous rocks failed to fully investigate the effective stress law within sandstones and their degree of compaction at a constant differential pressure while varying the pore fluid pressure. The results from the suite of experiments performed at a differential pressure of 20 MPa showed consistent enhanced compaction at higher pore fluid pressure, supporting the hypothesis that varying the pore fluid pressure would have an effect on the degree of compaction ad inelastic behavior. The experiments represented here from the suite performed at a differential pressure of 10 MPa had data demonstrating that the effective stress law is supported at a differential pressure of 10 MPa for Adamswiller sandstone.

Thin section analysis of the enhanced compaction at high pore fluid pressures at a differential pressure of 20 MPa showed less faulting, possibly from increased normal stress within the grain. Quantitative analysis of grain damage could elucidate a different reason behind the enhanced compaction and is an avenue of further research for the current Adamswiller sandstone samples.

Further work into the axial deformation of Adamswiller sandstone would investigate experiments performed at a higher differential pressure of 30 MPa to determine whether the enhanced compaction at a differential pressure of 20 MPa persists.

6. Acknowledgements

Thank you to Dr. Wenlu Zhu and Zachary Zega for assisting in writing and editing this paper, as well as helping me navigate the Rock Dynamics Laboratory and its instruments. Thanks to Dr. Philip Piccoli for assistance in editing this paper.

7. References

Brace, W. F. (1978). Volume changes during fracture and frictional sliding: A Review. *Rock Friction and Earthquake Prediction*, 603–614. https://doi.org/10.1007/978-3-0348-7182-2_3

Dropek, R. K., Johnson, J. N., & Walsh, J. B. (1978), The influence of pore pressure on the mechanical properties of Kayenta sandstone, *J. Geophys. Res.*, 83(B6), 2817– 2824, doi:10.1029/JB083iB06p02817.

Kranz, R. L. (1983). Microcracks in rocks: A Review. *Tectonophysics*, *100*(1-3), 449–480. https://doi.org/10.1016/0040-1951(83)90198-1

Menéndez, B., Zhu, W., & Wong, T.-F. (1996). Micromechanics of brittle faulting and cataclastic flow in berea sandstone. *Journal of Structural Geology*, *18*(1), 1–16. https://doi.org/10.1016/0191-8141(95)00076-p

Nur, A., & Byerlee, J. D. (1971). An exact effective stress law for elastic deformation of rock with fluids. *Journal of Geophysical Research*, *76*(26), 6414–6419. https://doi.org/10.1029/jb076i026p06414

Wong, T. F., & Baud, P. (1999). Mechanical compaction of Porous Sandstone. *Oil & Gas Science and Technology*, *54*(6), 715–727. https://doi.org/10.2516/ogst:1999061

Wong, T.F., & Baud, P. (2012). The brittle-ductile transition in Porous Rock: A Review. *Journal of Structural Geology*, *44*, 25–53. https://doi.org/10.1016/j.jsg.2012.07.010

Wong, T.F., David, C., & Zhu, W. (1997). The transition from brittle faulting to cataclastic flow in porous sandstones: Mechanical deformation. Journal of Geophysical Research: Solid Earth, 102(B2), 3009–3025. https://doi.org/10.1029/96jb03281

Worden, R. H., Armitage, P. J., Butcher, A. R., Churchill, J. M., Csoma, A. E., Hollis, C., Lander, R. H., & Omma, J. E. (2018). Petroleum Reservoir Quality Prediction: Overview and contrasting approaches from sandstone and carbonate communities. *Geological Society, London, Special Publications*, *435*(1), 1–31. https://doi.org/10.1144/sp435.21

Zhang, J., Wong, T.-F., Yanagidani, T., & Davis, D. M. (1990). Pressure-induced microcracking and grain crushing in Berea and Boise sandstones: Acoustic emission and quantitative microscopy measurements. *Mechanics of Materials*, *9*(1), 1–15. https://doi.org/10.1016/0167-6636(90)90026-c

Code of Conduct:

"I pledge on my honor that I have not given or received any unauthorized assistance or plagiarized on this assignment."